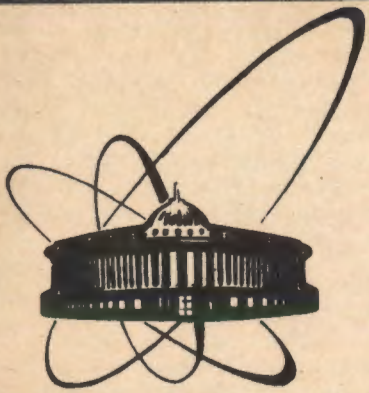

объединенный
институт
ядерных
исследований
дубна

E15-91-411

A.N.Andreyev, D.D.Bogdanov, V.I.Chepigin,
Ye.A.Cherepanov, A.P.Kabachenko, O.N.Malyshev,
K.V.Mikchajlov, Yu.A.Muzychka, G.S.Popeko,
B.I.Pustylnik, R.N.Sagaidak, G.M.Ter-Akopian,
A.V.Yeremin

STUDIES OF FORMATION OF FUSION EVAPORATION RESIDUES WITH $Z \geq 83$ IN HEAVY ION REACTIONS

Submitted to "International Symposium Nikko 91,
"Toward a Unified Pucture of Nuclear Dynamics",
Japan, 6-8 June, 1991

1991

measured production cross-sections to the element 110 nuclei gives for one of the most favourable reactions $^{208}Pb(^{62}Ni,1n)$ the value close to the subpicobarn region[13-15,19]. Considerations[19,20] based on the conception of the extra-extra push barrier[21] also leaved almost no room for optimistic evaluation of prospects of the new element synthesis by the cold fusion reactions.

The chances of the so-called hot fusion reactions are estimated to be even more pessimistic[19]. Unfortunately, studies of such reactions utilizing the target nuclei of actinide elements and bombarding ions of carbon, oxygen, neon etc. have been ceased since seventies (see ref.[22]) The lack of the experimental results about such asymmetric reactions is an obstacle to the more or less realistic evaluations of the cross sections for reactions which could be used for synthesizing the new heavy nuclides including the nuclei of new elements. Both, fusion cross-sections for asymmetric reactions and the survival probabilities of excited fissile compound nuclei are of interest. Bearing this in mind we initiated systematic studies of evaporation residues formation in the region of compound nuclei with atomic numbers $Z \geq 83$. We give in this paper some results of this work.

2. EXPERIMENTAL SET-UP

To carry out the experiments the U-400 cyclotron of the Laboratory of Nuclear Reactions, JINR, Dubna was used. The projectile beams were as follows: ^{20}Ne (120, 140 and 190 MeV), ^{22}Ne (110 and 130 MeV), ^{24}Mg (141 and 172 MeV), ^{26}Mg(136 and 164 MeV), ^{40}Ar (217, 250 and 293 MeV), ^{40}Ca (215, 228 and 270 MeV). The beam intensities passing through targets (12mm in diameter) were $(0.3-3.0)*10^{12} s^{-1}$ at an energy spread of (1-1.5)% . The beam energy was changed in 3-6 MeV steps using Al and Ti degraders. The energy of the beam was controlled by measuring the energy of ions scattered in a thin (200 $\mu g/cm^2$) gold foil at 30°.

To separate the evaporation residues of heavy-ion fusion reaction from the projectile beams and background products the kinematic separator VASSILISSA[23,24] was used. A schematic view of the separator is shown in fig.1. The evaporation residues knocked out from the target were separated by an achromatic system composed of three electric dipoles. Two triplets of electromagnetic quadrupole lenses provided the focusing on a detector system of recoil nuclei emerging from the target at zero angle within a solid angle of 10 msr. The distance from the target to the focal plane was about 12 m. The detector system consisted of two time-of-flight detectors and silicon detectors. Thin plastic foils emitting

secondary electrons and microchannel plates for detecting these electrons were exploited in start and stop time-of-flight detectors. The typical time resolution about 2 ns was obtained for slow (full energy 10-20 MeV) recoil nuclei having mass numbers of about 200. The value 99.95% was achieved for the probability of detection of such recoil nuclei by a single timing detector. After passing the time-of-flight system, recoil nuclei were implanted in silicon detectors which we took in the form of either an array of seven separate detectors or a single crystal divided into eight independent strips. The measurement of the time-of-flight and the energy of recoil nuclei provided their mass determination with an accuracy of about 5%. The whole system provided the uniform detection probability of recoil nuclei within an circular area of 70 mm in diameter.

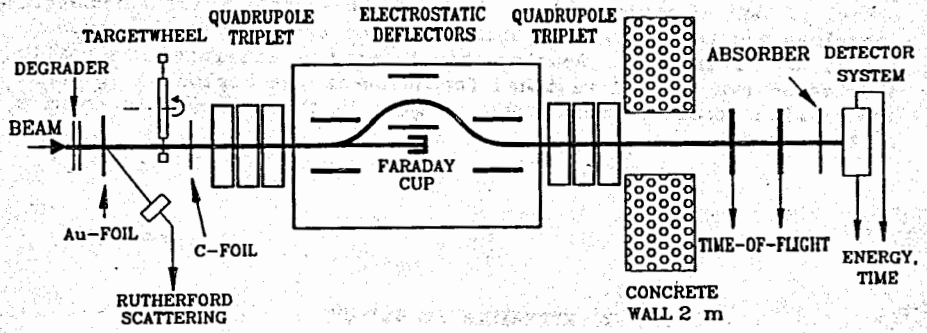

Fig. 1 Schematic view of the experimental set-up.

The heavy-ion fusion reaction products were unambiguously identified by the measured values of their α-decay energy and the life-times. In many cases the identification was performed due to observation of the time correlated α-decays of nuclides belonging to the known α-decay chains. This method was applied in each case when the identification of a previously unknown nuclide or an α-decay line was considered. In fig. 2 we show an example of two - dimensional spectrum of α-α correlation. Such correlations as well as the recoil-alpha time correlations were used for life-time measurements of investigated nuclides. Table I gives the values of measured transportation efficiencies of different evaporation residues from the target to

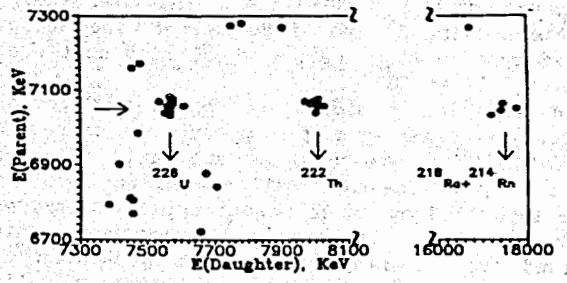

Fig. 2. An example of a two-dimensional α-α correlation plot obtained for reaction $^{26}Mg+^{208}Pb$ at a beam energy $E(^{26}Mg)=135$ MeV for the time window of 100-400 ms [27].

the detector system. We performed the measurements of such values taking targets of different thickness for a set of projectile-target combinations and for evaporation residues produced in xn or pxn as well as in αxn evaporation reactions. The transportation efficiencies of the evaporation residues for properly choosen control reactions were measured in all experiments. Therefore, the relative accuracy of cross section values deduced for a given target-projectile combination was about ±25%. For whole set of the data presented in this work the relative errors in the cross-sections are evaluated to be about ±50%. The errors due to uncertainty and inhomogeneity of the targets used in experiments constituted the negligible part of these errors. Only in few cases the errors were larger due to the poor statistic. The absolute values of the cross sections are probably accurate within factor of two due to errors in measurements of the beam current.

Table I. Experimental results for the separation efficiency

Reaction	Separation efficiency (%) target thickness	
	0.22 mg/cm^2	0.5 mg/cm^2
$^{197}Au(^{16}O,4\text{-}5n)^{208,209}Fr$	3±1	2±1
$^{182}W(^{22}Ne,4\text{-}5n)^{199m,199g,200}Po$	5±1	3±1
$^{166}Er(^{31}P,4n)^{193}Bi$	14±2	
$^{164}Dy(^{40}Ar,4\text{-}5n)^{199m,199g,200}Po$	25±3	19±3

We supposed that the detection efficiency of the α-decay of implanted nuclei was 50% for all reactions studied in this work.

One can evaluate the background conditions of the experiments taking the values of probabilities of passage through the separator to the detector system measured for projectile-like products and products of transfer reactions. These values are given in Table II.

Table II. The suppression factors for multi-nucleon transfer reaction products and for the scattered ions

Reaction	Target thickness, mg/cm^2	Suppression factors: Scattered ions	Transfer reaction products
$^{238}U+^{40}Ar$	0.5	$2\cdot10^{10}$	$2\cdot10^4$ (for ^{242}Cm) $8\cdot10^4$ (for ^{227}Th)
$^{208}Pb+^{40}Ar$	0.6	$2\cdot10^{10}$	$7\cdot10^3$ (for ^{211}Bi)
$^{248}Cm+^{22}Ne$	0.33	$3\cdot10^{12}$	$> 4\cdot10^3$ (for ^{254}Fm)

3. SOME FEATURES OF ASYMMETRIC FUSION REACTIONS LEADING TO THE FORMATION OF FISSILE COMPOUND NUCLEI WITH Z≥83

The list of heavy-ion fusion reactions studied in this work is given in Table III. For all of these reactions the xn evaporation channel was investigated in the range of bombarding energies extending from subbarrier values to the region corresponding to excitation energy of compound nuclei close to 100 MeV for the lighter (Z≥91) compound nuclei and about 50-60 MeV for heavier compound nuclei. Several new nuclides (or new α-lines) were obtained in the course of these experiments[25-29] (see Table IV). In addition to the xn evaporation channel, some data were obtained also for cross-sections of pxn and αxn reaction channels (see Table III). The row data were obtained in the form of excitation curves of fusion-evaporation reaction channels. Same examples of excitation curves are given in figures 3 and 4.

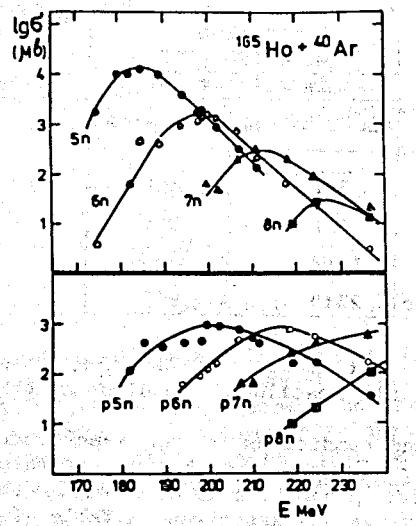

Fig.3. Excitation functions of the xn and pxn reaction channels in reaction ^{40}Ar+^{165}Ho.

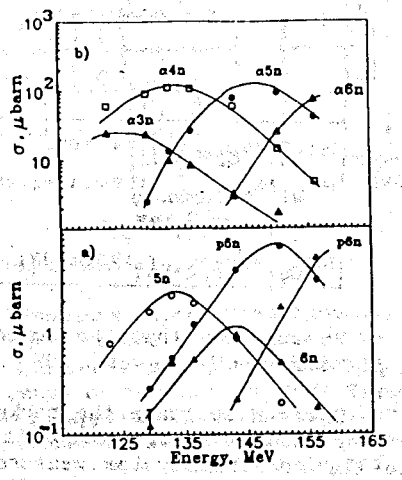

Fig.4. Excitation functions of the xn, pxn and αxn reaction channels in reaction ^{26}Mg+^{197}Au.

In fig.5 the systematics is given for the maximum values of xn-reaction cross sections obtained in this work. Similar results for compound nuclei of Ac and Th published by other authors[5,30] obtained with ^{48}Ca and ^{40}Ar bombarding ions are added to the data given in this figure. For comparison, we present in this figure the data for compound nuclei in the range of atomic numbers 98-104 measured by different authors who worked with bombarding ions of carbon, nitrogen, oxygen and neon (see references in the review paper[22]. The points in fig.5 represent the row experimental results for maximum values of measured cross-sections. We only excluded

the data for those reactions for which the maximum values of the cross-sections are strongly affected by the

Table III. The list of heavy-ions fusion reactions studied in this work

Reaction	Z_{CN}	A_{CN}	xn-channel		pxn-channel		αxn-channel	
			x_{min}	x_{max}	x_{min}	x_{max}	x_{min}	x_{max}
^{40}Ar+^{159}Tb	83	199	4	10				
^{40}Ca+^{153}Eu	83	193	3	6	3	5		
^{40}Ca+^{151}Eu	83	191	3	4	2	4		
^{26}Mg+^{181}Ta	85	207	4	7				
^{40}Ar+^{165}Ho	85	205	4	9	4	9		
^{24}Mg+^{181}Ta	85	205	4	9	4	9		
^{40}Ca+^{159}Tb	85	199	3		2	5	2	4
^{22}Ne ^{197}Au	89	219	3	7	3	7		
^{20}Ne+^{197}Au	89	217	4	8	4	9	4	9
^{22}Ne+^{205}Tl	91	227	3	6	3	5	2	4
^{26}Mg+^{197}Au	91	223	5	6	5	6	3	6
^{24}Mg+^{197}Au	91	221	3	6	3	7	4	5
^{22}Ne+^{208}Pb	92	230	4	5			2	4
^{20}Ne+^{208}Pb	92	228	4	5	4	5	2	4
^{22}Ne+^{209}Bi	93	231	4	5			2	4
^{26}Mg+^{208}Pb	94	234	4				2	3
^{22}Ne+^{236}U	102	258	4	6				
^{26}Mg+^{232}Th	102	258	4	6				

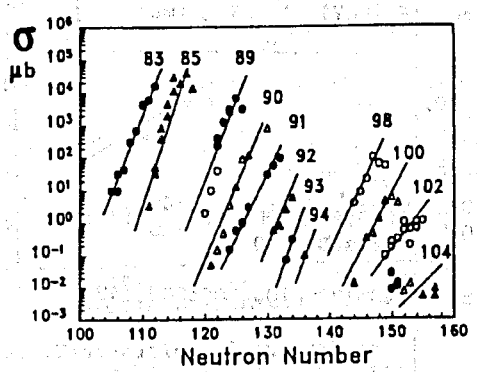

Fig.5 Systematics of the maximum values of the xn-reaction cross-sections. The circles and triangles alternate in order to facilitate the recognition of data obtained for evaporation residues having different atomic numbers. Our results are presented by closed symbols.

Coulomb barrier. We note that for Z≤ 91 the points are shown in this figure which represent, for given evaporation residues, the maximum cross-sections obtained with projectiles having rather different mass numbers (^{20,22}Ne, ^{24,26}Mg on the one side and ^{40}Ar, ^{40,48}Ca on the other). These point are drawn in figure without correction taking into account the $\pi\lambda^2$ factor. Some of evaporation residues were produced by different bombarding ions (i.e. ^{20}Ne and ^{22}Ne or ^{24}Mg and ^{26}Mg) as a result of evaporation of different numbers of neutrons. The points for all such reactions are presented in fig.5 without any corrections. Irrespective of these reservation, the points in fig.5 are grouped around the straight lines corresponding

to atomic numbers of evaporation residues. The slopes of these lines show the exponential decrease of xn reaction cross-sections with increasing deficit of neutrons in evaporation residues. This deficit aggravates the competition from the side of fission in the course of deexcitation of compound nuclei. Against the background of this steep exponential decrease the above-mentioned differences between some experimental points look to be of minor importance.

The analysis of experimental data on xn, pxn and αxn evaporation channels was based on the statistical model of the deexcitation process of compound nuclei. Calculations for compound nuclei from Bi to U were carried out using a modified version of the code ALICE. To describe the nuclear level density we used the relations of the Fermi gas model with the phenomenological consideration of shell effects in the level density parameter[31]. We assumed for the fission barrier the form

$$B_f(l)=C*B_f^{cps}(l)+\Delta B_f(Z,A), \qquad (1)$$

where $B_f^{cps}(l)$ is the fission barrier in the model of the rotating charged liquid droplet[32], C is the free parameter, $\Delta B_f(Z,A)$ is

Table IV. The alpha-decay characteristics of some nuclei, investigated in our experiments

	VASSILISSA			other works			
	E_α(keV)	I_α	$T_{1/2}$(ms)	E_α(keV)	I_α	$T_{1/2}$(ms)	
^{223}U	8780±40	100	$0.018^{+0.01}_{-0.005}$				
^{224}U	8470±15	100	$0.7^{+0.9}_{-0.2}$				
^{225}U	7870±20	100	30^{+20}_{-10}	7880±20	90	80^{+40}_{-20}	[41]
				7830±20	10		
^{226}U	7570±20	85±5	200±50	7430±20	100	500±200	[43]
	7420±20	15±5					
^{225}Np	8630±20	100	***				
^{226}Np	8000±20	50±15		8044±20	100	31±8	[42]
	8060±20	50±15					
^{227}Np	7680±20	100	(EC<25%)	7650±20		510±60	[42]
				7677±20			
^{230}Pu	7050±20	100					

*** preliminary data

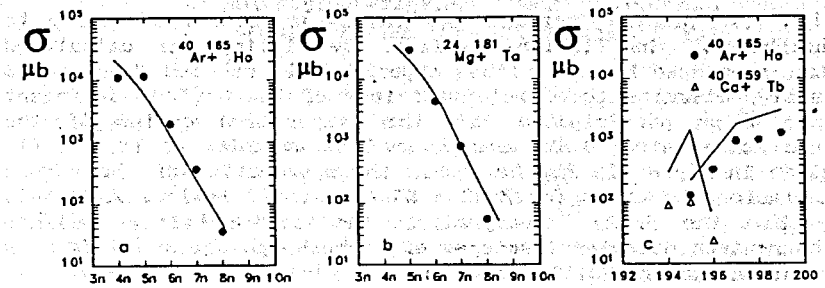

Fig. 6. Comparison of the experimental maximum values of the evaporation reaction cross-sections with calculations (solid line) for Z=85 compound nuclei[29]. a), b) - xn-channels, c) - pxn-channels.

the shell correction for the fission barrier of the compound nucleus. The nuclear potential and the choice of the critical value of the angular momentum (l_{cr}) for the compound nucleus formation were considered earlier[33].

The aim of our calculations was the optimum description of the maximum values of cross-sections well above the Coulomb barrier. Therefore, there was no need for additional variation of previously fitted parameters of nuclear potential[33]. More than 90% of cross-section values in their maxima are achieved at $l \ll l_{cr}$. For this reason, the results of calculations were not much sensitive to the value of l_{cr}. We found that calculations could not reproduce experimental results adequately only by variations of shell corrections to nuclear masses and fission barriers, as well as the excitation energy dependence of these values. At this stage we neglected the shell effects in our calculations. We note that there was no need in using the value of level density parameter (a_f) for fission channel different to that for particle evaporation channels (a_ν).

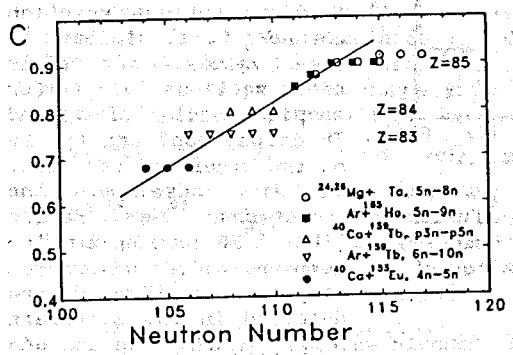

Fig. 7. Systematics of the values of parameter C (see, equation (1)) deduced for the neutron deficient isotopes of Bi, Po and At.

Thus, we came to the conclusion that the maximum values of evaporation reaction cross-sections could be fitted rather well by varying only one parameter of the model, i.e. the factor C in

equation (1). In other words, these values are rather sensitive to the heights of the fission barriers. By fitting the calculated maximum cross-sections to the experimental results one could eventually determine the fission barriers of the neutron deficient nuclides which participated in the evaporation chains of the compound nuclei studied in this work. Some examples of such a fit are given in fig.6. In fig.7 we show the systematics of the values of the factor C deduced for Z=83 - 85 nuclei. It follows from this figure that the theory[32] overpredicts the fission barrier heights for the neutron deficient isotopes of bismuth, polonium and astatin with neutron numbers N≤112.

Inspection of the data given in fig.5 reveals relatively weak dependence of the maximum cross-section values for compound nuclei lying in two intervals, i.e. Z=83 - 90 and Z=92 - 102 whereas the steep decrease is observed in transition from thorium to uranium. This feature of the cross-sections is seen clearly in fig.8 in which the data are shown for the reactions giving evaporation residues equally displaced from the β-stability line. Similar behaviour was obtained also for pxn and αxn reactions. However, the steep decrease obtained for αxn reactions is shifted in fig.8 to the transition from uranium to plutonium. This leads, in particular, to the fact that xn and αxn reaction channels are similar in the values of their cross-sections for compound nuclei of Ac and Th on one hand and for Pu on the other. In contrast, in the case of the reactions $^{22}Ne+^{208}Pb$ and $^{20}Ne+^{208}Pb$ leading to the compound nuclei of uranium the cross-sections were detected in the microbarn region for 4n and 5n reaction channels whereas for α2n, α3n and α4n reactions channels the obtained cross-section values were close to millibarns[25,28].

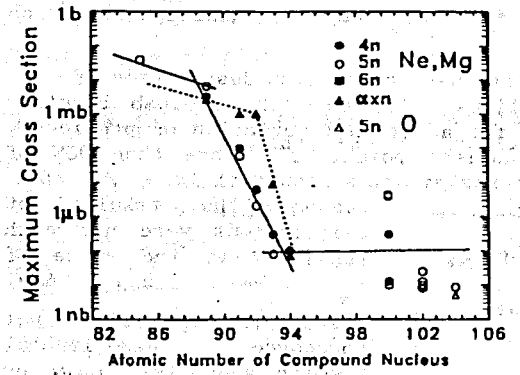

Fig.8. Maximum cross-section values for xn and αxn channels of fusion reactions giving evaporation residues equally displaced from the valley of β-stability.

It is difficult for us to outline any idea which could explain such cross-section behaviour as due to any limitation on the formation of uranium or plutonium compound nuclei. At the same time, the explanation of the obtained steep decrease of the evaporation reaction cross-sections on account of the high fissility of Z>90 nuclides appears to be quite natural. In fact, we could fit in our calculations all set of the results for Ac, Th, Pa and U nuclei presented in fig.5 as well as the data for pxn and αxn reactions by taking the following values for factor C in equation (1) : C=1 for Ac and Th; C=0.7 for Pa and C=0.65 for U nuclei.

4. HOT FUSION REACTIONS $^{22}Ne+^{236}U$ AND $^{26}Mg+^{232}Th$ LEADING TO THE COMPOUND NUCLEUS $^{258}102$.

The aim of the experiments was to obtain the new data about the formation of evaporation residues of the compound nucleus $^{258}102$. Earlier, three reactions, i.e. $^{12}C+^{246}Cm$[34], $^{15}N+^{243}Am$[35] and $^{16}O+^{242}Pu$[36] have been studied. Addition of two other reactions would complete this sequence of asymmetric hot fusion reactions leading to the same compound nucleus $^{258}102$. The variations of the mean arithmetical fissility parameter[21] along this sequence (see table 5) originates entirely from the difference in entrance channel configurations. Therefore, studies of these two reactions could shed some light on the problem of extra-extra push barrier for hot fusion reactions, which are of interest from point of view of possible synthesis of nuclides in the region of the neutron number 162. In fact, it is not excluded that bombarding ions of ^{22}Ne and ^{26}Mg could be used successfully in combinations with target nuclei of ^{248}Cm, ^{249}Bk and ^{249}Cf for synthesizing nuclides which belong to the predicted[37] stability island centered around this neutron number.

The experimental conditions were essentially the same as was described above. Three evaporation residues, i.e. isotopes of element 102 having the mass numbers 254, 253 and 252 were registered in focal plane of the separator. These isotopes emerging from 4n, 5n and 6n evaporation channels were identified through their characteristic α-decay lines. The 25% spontaneous fission decay branch of $^{252}102$ as well as α-decays of daughter nuclei of $^{252}102$ and $^{253}102$, i.e. ^{248}Fm and ^{249}Fm were detected.

The measured excitation curves of the studied reactions are shown in fig.9. We calculated the xn reaction cross-sections using the method described in Ref.[34,38,39]. Due to the fact that fission and neutron evaporation competition is treated in this approach by exploiting the empirical Γ_n/Γ_f systematics[40], one could simplify the analysis as Γ_n/Γ_f values were essentially the same for all reactions. Therefore, by comparing the experimental data with calculated cross-sections one could count on extracting some information about the fusion probability for different entrance channel configurations. Such a comparison is given in Table 5. We deduced the following conclusions from this table.

Table V. Maximum cross section values for neutron evaporation channels of the compound nucleus $^{258}102$

Reaction	x^{arith}_{mean}	Ref.	Cross section (nanobarn)					
			Experiment			Calculation		
			4n	5n	6n	4n	5n	6n
$^{12}C+^{246}Cm$	0.680	[34]	1000	300		227	107	22
$^{15}N+^{243}Am$	0.694	[35]	80			116	85	20
$^{16}O+^{242}Pu$	0.698	[36]	34	55		111	78	15
$^{22}Ne+^{236}U$	0.721	This work	7	25	15	74	64	9.2
$^{26}Mg+^{232}Th$	0.735	This work	1.5	9	8	42	46	8.2

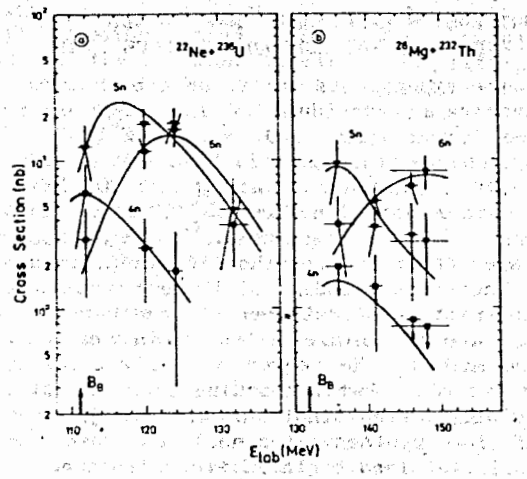

Fig.9. Excitation curves of neutron evaporation channels for the compound nucleus $^{258}102$.

The experimental maximum values of the cross-sections for the 4n and 5n evaporation channels are reproduced by calculations quite reasonably for the case of the three most asymmetric reactions. Some differences between experimental and calculated values not exceeding the factor of 4 are within the typical limits of the model accuracy[38,39]. The agreement is much worse in the case of the 4n channel obtained for heavier projectiles (^{22}Ne and, especially, ^{26}Mg). One could explain this as an indication of the onset of the extra-extra-push barrier at the transition from $^{16}O+^{242}Pu$ reaction to more symmetric ones, i.e. to $^{22}Ne+^{236}U$ and $^{26}Mg+^{232}Th$. Indeed, the agreement could be improved considerably by adding 5 MeV to the height of the Coulomb barrier for ^{26}Mg. However, we refrain from inferring any conclusion about the extra-extra-push barrier as 4n and 5n channels are strongly subbarrier for $^{22}Ne+^{236}U$ and $^{26}Mg+^{232}Th$ reactions, and we hardly can insist that our accuracy in the calculation of the barrier penetration is high enough.

At any rate, we regard the observation of an anomalously small value of 4n reaction cross-section in the case of ^{26}Mg (^{22}Ne) as an indication that this reaction channel has a little chance to be helpful in the synthesis of new heavy nuclides. Contrary to this, the 6n reaction cross-section does not tend to the drastic decrease for the case of heavy projectiles. Though with some reservations, this is also true for 5n reaction. Therefore, we suppose that these two reactions will be practical in the work on the synthesis of new heavy isotopes of elements 106-110 with the beams of ^{22}Ne and ^{26}Mg.

References

1. J.R.Nix and A.J.Sierk, Phys. Rev. C15, 2072 (1977).
2. W.J.Swiatecki, Phys. Scr. 24, 113 (1981).
3. S.Bjornholm and W.J.Swiatecki, Nucl. Phys. A391, 471 (1987).

4. H.Gaeggeler et al., Z.Phys. A316, 291 (1984).
5. C.-C.Sahm, H.-G.Clerc, K.-H.Schmidt, W.Reisdorf, P.Armbruster, F.P.Hessberger, J.G.Keller, G.Muenzenberg and D.Vermeulen, Nucl. Phys. A441, 316 (1985).
6. J.G.Keller, K.-H.Schmidt, F.P.Hessberger, G.Muenzenberg, W.Reisdorf H.-G.Clerc and C.-C.Sahm, Nucl. Phys. A452, 173 (1988).
7. W.Reisdorf, F.P.Hessberger, K.D.Hildenbrand, S.Hoffman, G.Muenzenberg, K.-H.Schmidt, W.F.W.Schneider, K.Suemerer, G.Wirth, J.V.Kratz, K.Schlitt and C.-C.Sahm, Nucl.Phys., A444, 154, (1985)
8. R.Bock et al., Nucl.Phys., A388, 334(1982).
9. W.Q.Shen, J.Albinski, A.Gobbi, S.Gralla, K.D.Hildenbrand, N.Herrmann, J.Kuzminski, W.F.J.Mueller, H.Stelzer, J.Toke, B.B.Back, S.Bjornholm and S.P.Sorensen, Phys.Rev.C36, 115, (1987)
10. B.B.Back, In : Int. School-Seminar on Heavy Ion Physics, Dubna, 1986; JINR D7-87-68 (Dubna, 1987), p. 465.
11. Yu.Ts.Oganessian, In : Int.School-Seminar on Heavy Ion Physics, Alushta, 1983; JINR D7-83-644 (Dubna, 1983), p.55.
12. Yu.Ts.Oganessian, M.Hussonnois, A.G.Demin, Yu.P.Kharitonov, H.Bruchertzeifer, O.Constantinescu, Yu.S.Korotkin, S.P.Tretyakova, V.K.Utyonkov, I.V.Shirokovsky and J.Estevez, Radiochimica Acta 37, 113 (1984).
13. P.Armbruster, Ann. Rev. Nucl. Part. Sci 35, 135 (1985).
14. G.Muenzenberg, Rep. Prog. Phys. 51, 57 (1988).
15. S.Hoffman, In : Int. School-Seminar on Heavy Ion Physics, Dubna, 1990, JINR, D7-90-142 (Dubna, 1990), p.338.
16. C.H.Dasso, J.Fernandez-Niello and S.Landowne, Phys. Rev. C41, 1014 (1990).
17. P.Moller, J.R.Nix and W.Swiatecki, Nucl. Phys. A469, 1 (1987).
18. P.Moller, J.R.Nix and W.Swiatecki, Nucl. Phys. A492, 349 (1989).
19. P.Armbruster, Varenna Course in Physics, 1987, Preprint GSI-87-9.
20. P.Armbruster, J. Phys. Soc. Jpn. 58, 232 (1989).
21. J.Blocki, H.Feldmeier and W.J.Swiatecki, Nucl. Phys. A459, 145 (1986).
22. G.N.Flerov and G.M.Ter-Akopian, Prog. Part. Nucl. Sci. 19, 197 (1987).
23. A.V.Yeremin et al., Nucl. Instr. & Meth. A274, 528 (1989).
24. A.N.Andreyev, D.D.Bogdanov, V.A.Gorshkov, A.V.Yeremin, A.P.Kabachenko, O.A.Orlova, G.M.Ter-Akopian, V.I.Chepigin, JINR, Rapid Communications, N3[29]-88 (Dubna, 1988), p.33.
25. A.N.Andreyev, D.D.Bogdanov, V.I.Chepigin, A.P.Kabachenko, O.A.Orlova, G.M.Ter-Akopian and A.V.Yeremin, Yad. Fiz. 50, n.9, 619, (1989) (in Russian).
26. A.N.Andreyev, D.D.Bogdanov, V.I.Chepigin, A.P.Kabachenko, S.Sharo, G.M.Ter-Akopian and A.V.Yeremin, Z. Phys. A337, 229 (1990).
27. A.N.Andreyev, D.D.Bogdanov, V.I.Chepigin, O.N.Malyshev, A.P.Kabachenko, S.Sharo, G.M.Ter-Akopian, A.V.Yeremin, Z. Phys. A337, 231, (1990).
28. A.N.Andreyev, D.D.Bogdanov, V.I.Chepigin, O.N.Malyshev, A.P.Kabachenko, G.M.Ter-Akopian and A.V.Yeremin, Z. Phys., A338, 363, (1991).
29. A.N.Andreyev, D.D.Bogdanov, V.I.Chepigin, A.P.Kabachenko,

Yu.A.Muzychka, O.A.Orlova, B.I.Pustylnik, G.M.Ter-Akopian, A.V.Yeremin, Yad. Fiz. 52, n.3(9),640,(1990) (in Russian).
30. D.Vermeulen, H.-G.Clerc, C.-C.Sahm, K.-H.Schmidt, J.G.Keller, G.Muenzenberg and W.Reisdorf, Z.Phys. A318,157,(1984).
31. A.V.Ignatjuk et al., Yad. Fiz. 21,485,(1975) (in Russian).
32. S.Cohen, P.Plasil and W.Swiatecki, Ann. Phys. 82, 557 (1974).
33. Yu.A.Muzychka and B.I.Pystylnik, In : Int. School-Seminar on Heavy Ion Physics, Alushta,1983. Preprint JINR, D3-83-644, (Dubna, 1983), p.420.
34. T. Sikkeland, A. Ghiorso and M. J. Nurmia, Phys.Rev.172,1232 (1968).
35. E.D.Donets, V. A. Shchegolev and V. A. Yermakov, Atomnaya Energiya 20, 223 (1966) (in Russian).
B. A. Zager, M. B. Miller, V. L. Mikheev, S. M. Polikanov, A. M. Sukhov, G. N. Flerov and L. P. Chelnokov Atomnaya Energiya 20, 230 (1966) (in Russian).
36. V. L. Mikheev, V. I. Ilyushchenko, M. B. Miller, S.M. Polikanov, G. N. Flerov and Yu. P. Kharitonov, Atomnaya Energiya 22, 90 (1967) (in Russian).
37. K. Böning, Z. Patyk, A. Sobiczewski and S. Cwiok, Z.Phys. A325, 479 (1986).
Z.Patyk and A.Sobiczewski, Preprint GSI-90-53, (Darmstadt, 1990).
38. T.Sikkeland et al., Phys. Rev. 169, 1000 (1968).
39. A.S.Iljinov, Yu.Ts.Oganessian and Ye.A.Cherepanov, Yad. Fiz. 36, n.1, 118 (1982) (in Russian).
40. Ye.A.Cherepanov, A.S.Iljinov and M.V.Mebel, J.Phys.G : Nuclear Phys. 9, 931 (1983).
41. F.P.Hessberger et al., Z. Phys. A333, 111 (1989).
42. V.Ninov et al., Z. Phys. A336, 473 (1990).
43. V.E.Viola et al., Nucl. Phys. A217, 372 (1973).

Received by Publishing Department
on September 10,1991.